ChemComm

COMMUNICATION

View Article Online
View Journal

Cite this: DOI: 10.1039/d6cc00738d

Received 3rd February 2026,
Accepted 28th May 2026

DOI: 10.1039/d6cc00738d

rsc.li/chemcomm

Multi-colour and red emissions from a small donor–acceptor molecule by breaching Kasha's rule

Prathaban G,[a] Akanksha Sharma,[b] Soumen De [b] and Susnata Pramanik *[a]

Reported herein is a small (MW 260 Da) organic molecule that emits multicolour and red lights, capitalising on simultaneous anti-Kasha and donor–acceptor effects. The molecule emits from two excited states, namely S_1 and S_3. Introduction of donor–acceptor substituents resulted in the large Stokes shifts (>5000 cm^{-1}) with negligible spectral overlap.

Multi-colour organic emitters are of great importance in real-life applications including multi-colour bioimaging, multi-colour display technologies, white light emissions, anti-counterfeiting, *etc.*[1] In particular, small organic fluorophores are highly desirable because of their improved cell permeability, reduced perturbation of biological function, and simplicity in solid-state device fabrication.[2] However, achieving broad colour tunability from blue to red within a single, low-molecular-weight molecule remains a formidable challenge. Most red-emissive organic systems rely on extensive π-conjugation or multiple donor–acceptor substitutions, frequently leading to high molecular weights (often ≥300 Da), diminished quantum yields, and predominantly single-colour emission.[3] Herein we describe a small organic molecule with a molecular weight of 260 Da that (i) emits red light in both solid and solution; (ii) produces multiple colours as a function of excitation wavelengths by breaching Kasha's rule and (iii) displays large Stokes shifts with little spectral overlap between absorption and emission bands. Such multifaceted properties from a single yet small molecule are unique and represent a noteworthy advance in molecular photophysics.

The design of this molecule stemmed from two basic concepts: first, the presence of an acenaphthylene core, which exhibits anti-Kasha emission[4] and second, the strategic installation of donor–acceptor substituents on opposite sides of the acenaphthylene core to obtain red-shifted emission[5] and large Stokes shifts,[6] which would lead to poor overlap between absorption and emission bands.[7] Furthermore, realising anti-Kasha emissions from a donor–π–acceptor (D–π–A) architecture is particularly appealing, as such systems hold promise for advanced applications, including ratiometric bioimaging, detection of cellular microenvironments, photodynamic therapy, *etc.*[8]

Recently, we reported vicinal diones like, acenaphthylene-1,2-dione, phenanthrene-9,10-dione, and pyrene-4,5-dione and their derivatives that can disobey Kasha's rule and emit from multiple excited states,[9] leading to multi-colour and even white light emissions.[10] However, these emissions were largely confined to the green-yellow region (~550 nm). To extend the emission into the red region, we designed compound **3** comprising an electron donor substituent (OMe) at one end of the acenaphthylene-1,2-dione and to make the other side a better acceptor, one of the carbonyl groups was reacted with malononitrile (Fig. 1a). For comparison, analogues bearing an electron-withdrawing nitro group (**2**) and no substituent (**1**) were also synthesised. These molecules display two emission bands, one in the blue region and another in the yellow to red (based on the substituents). The effect of substituents is clearly visible in their longer wavelength emissions; compound **3** emits in the most red-shifted region, while that of **2** in the most blue-shifted

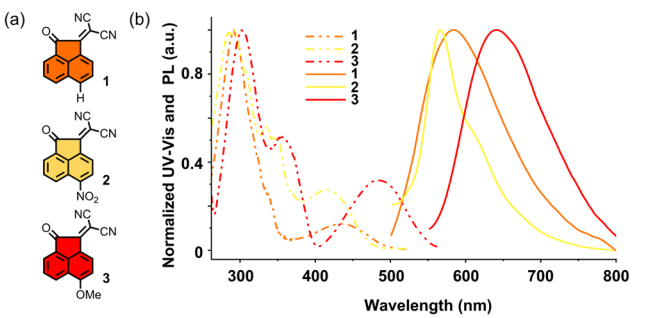

Fig. 1 (a) Chemical structure of compounds **1–3** and (b) normalized absorption (dotted line) and PL (solid line, $\lambda_{ex} = \lambda_{max}$, Table 1) in ACN at 10^{-5} M.

[a] *Department of Chemistry, Faculty of Engineering and Technology, SRM Institute of Science and Technology, Kattankulathur, Chennai, Tamil Nadu 603203, India. E-mail: susmatap@srmist.edu.in*

[b] *School of Chemistry, Indian Institute of Science Education and Research (IISER), Thiruvananthapuram, Kerala 695551, India*

region. Compound **1** exhibited emission that fell in between **2** and **3**. Interestingly, the high-energy emission bands did not display any substituents effects, implying that the emission may solely originate from the acenaphthylene core. This clear separation of emissive underpins the excitation-dependent multicolour behaviour observed in these compact molecules.

The synthesis of these derivatives and characterisation are presented in the SI, and the purity was confirmed using high-performance liquid chromatography (HPLC) (SI, Fig. S1–S10) and elemental analysis.[11] Single crystal structures of compounds **1** and **3**, and HRMS further confirm the integrity of these molecules (SI, Fig. S32 and S33).

Their absorption spectra revealed that compounds **1–3** possess three absorption bands (Fig. 1b). While compound **3** absorbs in the most red-shifted region (λ_{ab} = 482 nm), compound **2** exhibited the most blue-shifted absorption bands (λ_{ab} = 414 nm), and the same for **1** appeared to be in between (λ_{ab} = 435 nm), clearly indicating a strong substituents effect. Interestingly, all the compounds showed minimal solvatochromism in solvents of different polarities (Fig. S17–S19); the absorption maxima slightly red-shifted for compounds **1** and **3**, indicating that the excited state is more polar compared to the ground state. This, however, is not true for **2**; the absorption band at 414 nm undergoes hypsochromic shifts, implying that the ground state is more polar compared to the excited state.[12] Next, we recorded their emission spectra in acetonitrile ($c = 10^{-5}$ M, Fig. 1b, Table 1). Excitation (λ_{ex} = 435 nm) of **1** resulted in an emission band at 587 nm (ϕ_{PL} = 5.56 ± 0.31%, τ_{PL} = 5.37 ± 0.10 ns). However, for **2** (λ_{ex} = 414 nm), the emission band shifted towards blue and appeared at 567 nm (ϕ_{PL} = 1.14 ± 0.29%, τ_{PL} = 1.67 ± 0.04 ns). As expected, **3** exhibited the most red-shifted emission band at 642 nm (ϕ_{PL} = 2.84 ± 0.39%, τ_{PL} = 1.41 ± 0.12 ns, λ_{ex} = 482 nm).[13] These data indicate the effect of the donor–acceptor system in a small molecule to shift the emission wavelength into the red region. Interestingly, all three molecules exhibit large Stokes shifts of over 5000 cm^{-1} with the largest value of 6520 cm^{-1} for compound **2**, resulting in a negligible spectral overlap (SI Table S1).

As the molecules exhibit multiple absorption bands, we decided to excite them at different wavelengths to investigate their possible anti-Kasha effects. Excitation (λ_{ex} = 310 nm) of **1** resulted a in a strong emission band at 425 nm along with a band at 587 nm (Fig. 2a and d). However, the latter became the sole emission band at λ_{ex} = 440 nm. This resulted in the emission colours that ranging from blue to yellow. Similarly, compound **2** exhibited two emission bands at 425 nm and 567 nm when the excitation wavelengths were tuned: yielding colours that changing from blue to orangish-yellow (Fig. 2b and e). Not surprisingly, compound **3** was found to display excitation wavelength-dependent emissions; the shorter wavelength emission was observed at 426 nm while the longer wavelength emission was at 642 nm, illuminating colours from blue to red (Fig. 2c and f). These data clearly indicated that the high energy emission is independent of substituents ($\Delta\lambda_{em}$ = 1 nm) and primarily involved core-to-core electronic transition, while the red-shifted emission band is highly substituent dependent ($\Delta\lambda_{em}$ = 75 nm). The excitation spectra recorded for each of these emission bands clearly indicated that compounds **1–3** may emit from multiple excited states by breaching Kasha's rule (SI, Fig. S12–S14). Furthermore, the lifetimes and quantum yields for these emission bands are different, confirming that they originated from

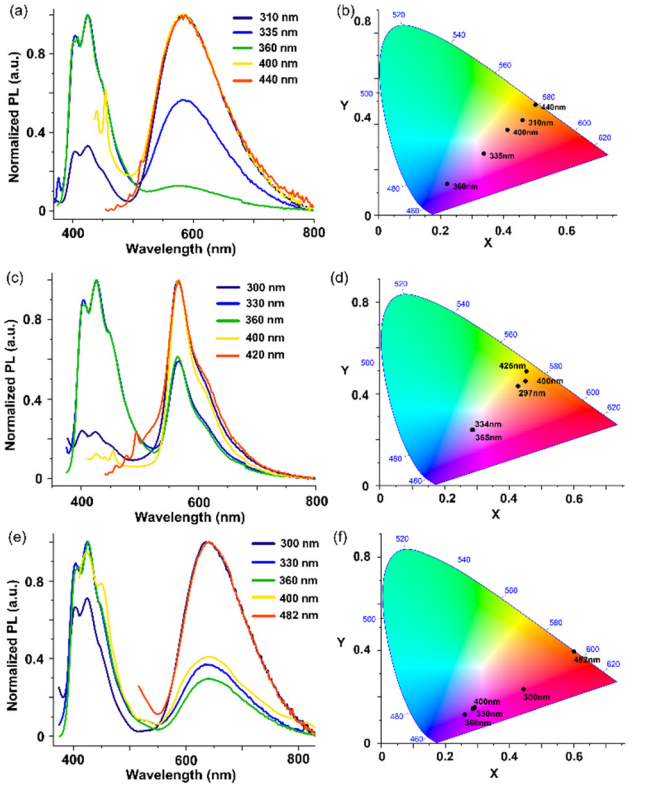

Fig. 2 Excitation wavelength-dependent emission studies of compounds (a) **1**, (b) **2** and (c) **3** and their corresponding CIE plots (d) **1**, (e) **2** and (f) **3** in ACN at 10^{-5} M.

Table 1 Photophysical properties of compounds **1–3** in solution

Compound[a]	$\lambda_{abs.}$[b] (nm)	λ_{em}[c] (nm)	τ_{FL}[d] (ns)	Φ_{FL}[e] (%)	λ_{em}[f] (nm)	τ_{FL}[g] (ns)	Φ_{FL}[h] (%)
1	435	425	1.61 ± 0.01	7.45 ± 0.21	587	5.37 ± 0.10	5.56 ± 0.31
2	414	425	1.27 ± 0.23	2.64 ± 0.39	567	1.67 ± 0.04	1.14 ± 0.29
3	482	426	1.57 ± 0.03	5.15 ± 0.19	642	1.41 ± 0.12	2.84 ± 0.30

[a] Photophysical studies were measured in ACN at $c = 10^{-5}$ M. [b] Absorption maxima of all three compounds. [c] Emission data recorded for all three compounds at λ_{ex} = 360 nm. [d] Lifetimes (λ_{ex} = 340 nm) of compounds **1–3** for high energy emission bands. [e] Relative PLQYs of compounds **1–3** for high energy emission bands. [f] Emission maxima recorded at $\lambda_{ex(1)}$ = 435 nm, $\lambda_{ex(2)}$ = 414 nm and $\lambda_{ex(3)}$ = 482 nm. [g] Lifetimes (λ_{ex} = 450 nm) of compounds **1–3** for low energy emission bands. [h] Relative PLQYs of compounds **1–3** for low energy emission bands.

different excited states (Table 1, SI, Fig. S23–S25). To further prove that the two emission bands were not originating from impurities, 2D excitation–emission correlation diagrams were plotted for all the compounds. A strong correlation between the emission bands indeed supports that the emissions originate from the same compounds (SI, Fig. S12–S14).[14]

Interestingly, all three molecules exhibited strong solvatochromism, resulting in a dramatic change in their emission behaviour (Fig. 3, SI, Fig. S17–S19). For example, for compound **1**, the λ_{em} = 425 nm band did not show any shifts but changed its intensity upon changing the polarity (Fig. 3a and b). On the contrary, the red-shifted emission band (λ_{em} = 587 nm) showed significant shifts and increased in intensity, indicating a strong charge-transfer character and the stabilisation of the excited state in polar solvents, which is in accordance with the absorption studies. Consequently, a wide range of colour tunability from blue to orangish-yellow, including near-white light (DCM, CIE coordinates 0.27, 0.28) was observed (SI, Fig. S17). By contrast, for compound **3**, the intensity of the λ_{em} = 642 nm band dramatically reduced accompanied by the red shifts in more polar solvents (Fig. 3e and f). This could be due to the stabilization of the excited state along with the opening of a non-radiative channel, possibly by the rotation of the methoxy group.[15] Nevertheless, it showed a nice colour tunability in various solvents from blue to orange (SI, Fig. S19). Solvatochromism was also demonstrated by compound **2**. As the solvent polarity increased, the emission peak at 567 nm shifted towards blue, suggesting that the ground state is more polar and stabilised by the polar solvents (Fig. 3c and d). It is unclear, nevertheless, why the emission intensity significantly decreased at λ_{em} = 425 nm. Overall, all three derivatives exhibited a charge transfer character of their low energy emission band, and for compounds **1** and **3** the excited state is more polar, while for **2**, it is the ground state.

Finally, the solid-state emissions of these new molecules were recorded. Interestingly, the changing of excitation energy did not result in the multiple emission bands, a common feature of molecules that obey Kasha's rule. This can be explained from the crystal structure of compounds **1** and **3** (Fig. 4a). The very short intermolecular distance, through π–π stacking, speeds up the rate of IC from the higher excited state(s), yielding emission only from the lowest excited state (*i.e.* S_1). Nevertheless, compounds **1** and **3** exhibited significant red shifts (595 nm and 673 nm, respectively) in their solid state compared to solution state emission (Fig. 4b). On the contrary, compound **2** displayed blue shifts (535 nm) in its solid-state emission. Although the aggregation-induced emission[16] (*i.e.* in the solid state) often resulted in bathochromic shifts, the hypsochromic shifts for **2** can be possibly attributed to the smaller reorganisation energy in the solid state compared to its solution state.[17] Nevertheless, **3** yielded red light in its solid state.[18]

To understand the photophysical behaviour of these compounds, we performed geometry optimisation and calculated their absorption and emission spectra using PBE functional and 6-311+g(d,p) basis set.[19] The highest occupied molecular orbitals (HOMO) of all compounds reside on the aromatic core and partly on the substituents, while that of the lowest unoccupied molecular orbitals (LUMO) is on the carbonyl and malononitrile segments, which are largely separated, and thus, indicates a charge transfer nature of electronic transitions between the HOMO and LUMO (Fig. 4d, SI, Fig. S34). The calculated absorption spectra revealed that the electronic transitions occurred from S_0 to S_1, S_3, S_4 and S_5 (S_2 is a dark state), resulting in the multiple bands in the electronic absorption spectra. However, the emission spectra, on the other hand,

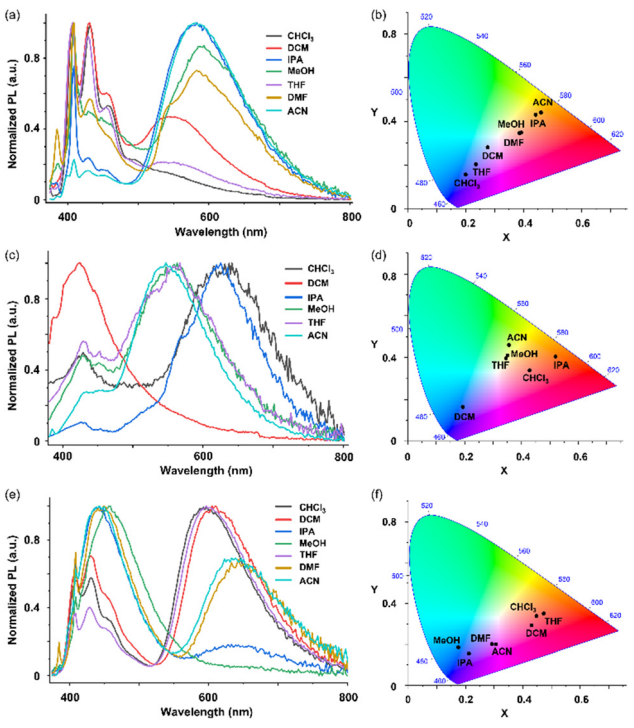

Fig. 3 Emission studies of compounds **1–3** in solvents of different polarities. (a), (c) and (d) Are normalized emission spectra, and (b), (d) and (f) are the corresponding CIE plots of **1**, **2** and **3**, respectively. λ_{ex} = 365 nm for all compounds.

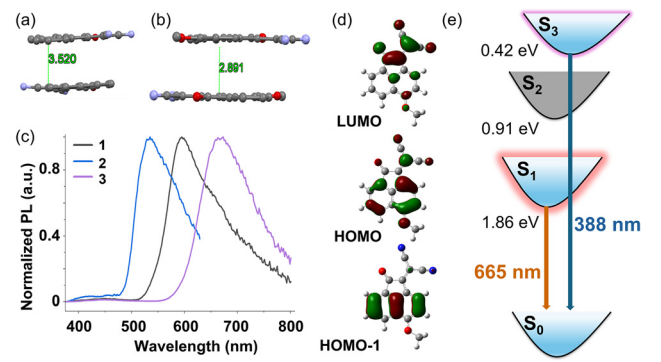

Fig. 4 Solid state packing of compounds (a) **1** and (b) **3** displaying their intermolecular distances. (c) Solid state fluorescence spectra of compounds **1–3** (λ_{ex} = 365 nm). (d) Calculated natural transition orbitals (NTOs) of compounds **3** using PBE functional and 6-311+g(d,p) basis set for $S_0 \rightarrow S_1$ absorption and (e) calculated emissive states of compound **3**. The energy levels are reported from the optimised S_1 state.

showed two relaxation processes, $S_3 \rightarrow S_0$ (blue-shifted band) and $S_1 \rightarrow S_0$ (red-shifted band), which involve HOMO−1 → LUMO and HOMO → LUMO electronic transitions, respectively (SI Tables S8–S13). As depicted in Fig. 4d, all the transitions are $\pi^* \rightarrow \pi$ types. Furthermore, although the substituents' contribution to the HOMO orbitals is noticeable in all compounds, the HOMO−1 orbitals lack it entirely. Consequently, there will be strong substituent effects in the low-energy emission band. On the other hand, the high-energy emission band may not exhibit a substituent effect, consistent with the experimental results. Additionally, the dipole moments in the ground state of the optimised structures are relatively high for compounds **1** and **3** (11.13 D and 12.94 D, respectively), and they are increased in the first excited state to 12.41 D and 15.09 D, respectively. On the contrary, the dipole moment in the ground state of **2** is low (only 5.61 D), while the same is marginally reduced to 5.17 in the first excited state. These data also support the experimental data, suggesting that the first excited state is more polar for **1** and **3** and possesses strong charge transfer character, while the ground state is more polar for **2** and may not display significant charge transfer character.

The calculated emission spectra of **3** revealed that the S_1 and S_3 are the bright state that emit in the visible range (Fig. 4e). The energy differences between S_1 and S_2 and S_2 and S_3 are 0.91 eV and 0.42 eV, respectively. Fluorescence from higher excited states is made possible by a relatively large $\Delta E_{S_3-S_2}$, which essentially lowers the rate of IC. Remarkably, S_2 was found to be a dark state with a zero oscillator strength. This makes us believe that the blue-shifted emission possibly occurs from S_3, which perfectly matches with that of the experimental data ($\lambda_{em(calc.)}$ = 388 nm, $\lambda_{em(expt.)}$ = 426 nm). This is also true for the low energy emission band ($\lambda_{em(calc.)}$ = 665 nm, $\lambda_{em(expt.)}$ = 642 nm) that originates from S_1 (Fig. 4e). The calculated emission spectra also agreed well for the compounds **1** and **2**. Thus, it is evident from both experimental and theoretical data that the malononitrile-substituted acenaphthylene diones violate Kasha's rule by emitting from two distinct excited states.

In summary, we report three donor–acceptor small organic molecules that emit in the red region with large Stokes shifts yet without affecting the anti-Kasha emissions. TDDFT calculations support the presence of two bright states, namely S_1 and S_3 resulting in a nice colour tunability from blue to red as a function of excitation wavelength. Additionally, the introduction of donor–acceptor substituents yielded red-emitting species , like **3**, as evidenced by the molecular orbital distribution on the acenaphthylene core. Consequently, this study will pave the way towards the development of multi-coloured and red emissive small molecules that can be useful in various fields, including multi-colour OLEDs, anticounterfeiting, bioimaging and photodynamic therapy.[20]

Conflicts of interest

There are no conflicts to declare.

Data availability

CCDC 2528322 and 2528323 contain the supplementary crystallographic data for this paper.[21a,b]

The data supporting this paper have been included as part of the supplementary information (SI). Supplementary information: detailed synthetic procedure, characterization, necessary spectra, and theoretical data. See DOI: https://doi.org/10.1039/d6cc00738d.

Acknowledgements

S. P. acknowledges the SRM Institute of Science and Technology for providing instrumental facilities and Nanotechnology Research Center (NRC), SRMIST for single crystal X-ray diffractometer facility. This work is financially supported by DST-SERB, India (no. SRG/2021/001033). P. G. is grateful to SRMIST for fellowships. S. D. and A. S. acknowledge IISER Thiruvananthapuram for facilities.

References

1 (*a*) L. Xiao, Y. Xu, M. Yan, D. Galipeau, X. Peng and X. Yan, *J. Phys. Chem. A*, 2010, **114**, 9090–9097; (*b*) X. Yu, H. Zhang and J. Yu, *Aggregate*, 2021, **2**, 20–34; (*c*) X. Li, W. Zhou, Y. Liu, M. Hou, G. Feng, Y. Ji, Y. Zhang and G. Xing, *Chem. Commun.*, 2022, **58**, 11547–11550; (*d*) Z. Tao, G. Hong, C. Shinji, C. Chen, S. Diao, A. L. Antaris, B. Zhang, Y. Zou and H. Dai, *Angew. Chem., Int. Ed.*, 2013, **52**, 13002–13006; (*e*) G. Hong, A. L. Antaris and H. Dai, *Nat. Biomed. Eng.*, 2017, **1**, 0010; (*f*) X. Cai and B. Liu, *Angew. Chem., Int. Ed.*, 2020, **59**, 9868–9886; (*g*) D. Qu, M. Zheng, J. Li, Z. Xie and Z. Sun, *Light: Sci. Appl.*, 2015, **4**, e364; (*h*) W. Yao, Q. Tian and W. Wu, *Adv. Opt. Mater.*, 2019, **7**, 1801171; (*i*) J. Zhao, D. Jin, E. P. Schartner, Y. Lu, Y. Liu, A. V. Zvyagin, L. Zhang, J. M. Dawes, P. Xi, J. A. Piper, E. M. Goldys and T. M. Monro, *Nat. Nanotechnol.*, 2013, **8**, 729–734; (*j*) P. O. Anikeeva, J. E. Halpert, M. G. Bawendi and V. Bulović, *Nano Lett.*, 2009, **9**, 2532–2536.

2 (*a*) J. Chan, S. C. Dodani and C. J. Chang, *Nat. Chem.*, 2012, **4**, 973–984; (*b*) M. Vendrell, D. Zhai, J. C. Er and Y. T. Chang, *Chem. Rev.*, 2012, **112**, 4391–4420; (*c*) Y. Hong, J. W. Y. Lam and B. Z. Tang, *Chem. Soc. Rev.*, 2011, **40**, 5361–5388; (*d*) S. Wang, X. Yan, Z. Cheng, H. Zhang, Y. Liu and Y. Wang, *Angew. Chem., Int. Ed.*, 2015, **54**, 13068–13072; (*e*) Y. Wang, J. Kublitski, S. Xing, F. Dollinger, D. Spoltore, J. Benduhn and K. Leo, *Mater. Horiz.*, 2022, **9**, 220–251; (*f*) M. Sawatzki-Park, S.-J. Wang, H. Kleemann and K. Leo, *Chem. Rev.*, 2023, **123**, 8232–8250.

3 (*a*) M. Shimizu, Y. Takeda, M. Higashi and T. Hiyama, *Angew. Chem., Int. Ed.*, 2009, **48**, 3653–3656; (*b*) T. Beppu, K. Tomiguchi, A. Masuhara, Y.-J. Pu and H. Katagiri, *Angew. Chem., Int. Ed.*, 2015, **54**, 7332–7335; (*c*) B. Tang, C. Wang, Y. Wang and H. Zhang, *Angew. Chem., Int. Ed.*, 2017, **56**, 12543–12547; (*d*) R. Huang, B. Liu, C. Wang, Y. Wang and H. Zhang, *J. Phys. Chem. C*, 2018, **122**, 10510–10518; (*e*) B. Liu, Q. Di, W. Liu, C. Wang, Y. Wang and H. Zhang, *J. Phys. Chem. Lett.*, 2019, **10**, 1437–1442; (*f*) M. Mandal, T. Chatterjee, D. Roy, A. Das, C. K. De, S. Mandal, S. Ghosh, A. Sen, M. Ta and P. K. Mandal, *J. Phys. Chem. C*, 2020, **124**, 27049–27054; (*g*) H. Kim, W. Park, Y. Kim, M. Filatov, C. H. Choi and D. Lee, *Nat. Commun.*, 2021, **12**, 5409; (*h*) L. Lan and H. Zhang, *Angew. Chem., Int. Ed.*, 2025, **64**, e202509140; (*i*) R. Huang, Q. Qiao, D. Seah, T. Shen, X. Wu, F. de Moliner, C. Wang, N. Ding, W. Chi, H. Sun, M. Vendrell, Z. Xu, Y. Fang and X. Liu, *J. Am. Chem. Soc.*, 2025, **147**, 5258–5268.

4 (*a*) M. Kasha, *Discuss. Faraday Soc.*, 1950, **9**, 14–19; (*b*) H. Qian, M. E. Cousins, E. H. Horak, A. Wakefield, M. D. Liptak and I. Aprahamian, *Nat. Chem.*, 2017, **9**, 83–87; (*c*) J. Wang, X. Gu, H. Ma, Q. Peng, X. Huang, X. Zheng, S. H. P. Sung, G. Shan, J. W. Y. Lam, Z. Shuai and B. Z. Tang, *Nat. Commun.*, 2018, **9**, 2963; (*d*) B. Shao, N. Stankewitz, J. A. Morris, M. D. Liptak and I. Aprahamian, *Chem. Commun.*, 2019, **5**, 9551–9554; (*e*) X. Ma, L. Jia, B. Yang, J. Li, W. Huang, D. Wu and W.-Y. Wong, *J. Mater. Chem. C*, 2020, **9**, 727–735; (*f*) H.-T. Feng, J. Zeng, P.-A. Yin, X.-D. Wang, Q. Peng,

Z. Zhao, J. W. Y. Lam and B. Z. Tang, *Nat. Commun.*, 2020, **11**, 2617; (*g*) H. Wang, J. Wang, T. Zhang, Z. Xie, X. Zhang, H. Sun, Y. Xiao, T. Yu and W. Huang, *J. Mater. Chem. C*, 2021, **9**, 10154–10172; (*h*) M. Du, Y. Shi, Q. Zhou, Z. Yin, L. Chen, Y. Shu, G. Sun, G. Zhang, Q. Peng and D. Zhang, *Adv. Sci.*, 2021, **9**, 202104539; (*i*) X. Bi, Y. Shi, T. Peng, S. Yue, F. Wang, L. Zheng and Q. Cao, *Adv. Funct. Mater.*, 2021, **31**, 2101312.

5 (*a*) B. Sk, S. Khodia and A. Patra, *Chem. Commun.*, 2018, **54**, 1786–1789; (*b*) F. Ye, W. Chen, Y. Pan, S. H. Liu and J. Yin, *Dyes Pigm.*, 2019, **171**, 107746; (*c*) Y. Sugihara, N. Inai, M. Taki, T. Baumgartner, R. Kawakami, T. Saitou, T. Imamura, T. Yanai and S. Yamaguchi, *Chem. Sci.*, 2021, **12**, 6333–6341; (*d*) Z. Lei and F. Zhang, *Angew. Chem., Int. Ed.*, 2021, **60**, 16294–16308; (*e*) H. Piwoński, S. Nozue and S. Habuchi, *ACS Nanosci. Au*, 2022, **2**, 253–283; (*f*) C. S. Abeywickrama, *Chem. Commun.*, 2022, **58**, 9855–9869; (*g*) T. Zhang, X. Qu, J. Shao and X. Dong, *Chem. Soc. Rev.*, 2025, **54**, 8406–8433.

6 (*a*) H. Liu, G. Jiang, G. Ke, T.-B. Ren and L. Yuan, *ChemPhotoChem*, 2004, **8**, e202300277; (*b*) N. N. M. Y. Chan, A. Idris, Z. H. Z. Abidin, H. A. Tajuddina and Z. Abdullah, *RSC Adv.*, 2021, **11**, 13409–13445; (*c*) S. Wu, Z. Ban, H. Tang, N. Ma, X. Ran, Q. Zhou, Y. Zhang, Z. Wang and X. Yu, *Chem. Commun.*, 2025, **61**, 10574–10577.

7 (*a*) A. Dhara, T. Sadhukhan, E. G. Sheetz, A. H. Olsson, K. Raghavachari and A. H. Flood, *J. Am. Chem. Soc.*, 2020, **142**, 12167–12180; (*b*) I. Likhotkin, R. Lincoln, M. L. Bossi, A. N. Butkevich and S. W. Hell, *J. Am. Chem. Soc.*, 2023, **145**, 1530–1534.

8 (*a*) L. Shi, C. Yan, Z. Guo, W. Chi, J. Wei, W. Liu, X. Liu, H. Tian and W.-H. Zhu, *Nat. Commun.*, 2020, **11**, 793; (*b*) H. Wang, J. Wang, T. Zhang, Z. Xie, X. Zhang, H. Sun, Y. Xiao, T. Yu and W. Huang, *J. Mater. Chem. C*, 2021, **9**, 10154–10172; (*c*) X. Gu, X. Zhang, Y. Han, J. Mei, Q.-W. Zhang and J. Hua, *Chem. Sci.*, 2025, **16**, 16168–16179.

9 (*a*) N. Kumar, D. L. Lyngkhoi, S. Gaikwad, D. Samanta, S. Khatua and S. Pramanik, *New J. Chem.*, 2023, **47**, 15066–15075; (*b*) N. M. Kumar, D. L. Lyngkhoi, S. Gaikwad, J. Samanta, R. Ahamed, S. Khatua and S. Pramanik, *Chem. Commun.*, 2023, **59**, 14122–14125; (*c*) R. Srithar, J. Venkatesh, J. Saravanan, K. Muthu and S. Pramanik, *ChemPhotoChem*, 2025, **9**, e202500137; (*d*) R. Srithar, N. M. Kumar, R. Benny, S. Gaikwad, S. De and S. Pramanik, *Chem. – Eur. J.*, 2025, **31**, e02168.

10 J. Venkatesh, R. Srithar and S. Pramanik, *Chem. Commun.*, 2025, **61**, 15254–15257.

11 Compound **2** comprises 2.4% impurities as observed in ^{1}H NMR and HPLC analysis. We could not isolate pure **2** due to overlapping peaks in HPLC and the absence of a distinct TLC separation. It is most likely a structural isomer formed during synthesis, consistent with excellent elemental analysis results. All three compounds show similar dual emission behaviour and despite differing impurity levels no additional emission bands are observed in compound **2**. Thus, the impurity is unlikely to contribute significantly to the observed photophysical properties.

12 (*a*) D. S. Biradar, B. Siddlingeshwar and S. M. Hanagodimath, *J. Mol. Struct.*, 2008, **875**, 108–112; (*b*) B. Prusti and M. Chakravarty, *Dyes Pigm.*, 2020, **181**, 108543.

13 The short lifetime for compound **2** can be attributed to the fast intersystem crossing (ISC) which is observed for nitro-compounds (W. Rodríguez-Córdoba, L. Gutiérrez-Arzaluz, F. CortésGuzmán and J. Peon, *Chem. Commun.*, 2021, **57**, 1221812235; P. B. Ghosh and M. W. Whitehouse, *J. Med. Chem.*, 1968, **11**, 305–311). Similarly, presence of methoxy substituent in **3** can open nonradiative decay channel (through its free rotation) which resulted in low quantum yield and short lifetime.

14 To verify that one of the dual emissions is not originated from the impurity of the starting materials, photophysical studies were conducted for all the precursors. They indeed displayed dual emissions but in different wavelengths (Fig. S15 and S16).

15 I. A. Z. Al-Ansari, *J. Phys. Chem. A*, 2018, **122**, 1838–1854.

16 J. Mei, N. L. C. Leung, R. T. K. Kwok, J. W. Y. Lam and B. Z. Tang, *Chem. Rev.*, 2015, **115**, 11718–11940.

17 Q. Wu, T. Zhang, Q. Peng, D. Wanga and Z. Shuai, *Phys. Chem. Chem. Phys.*, 2014, **16**, 5545–5552.

18 Although single emission band was observed for all the compounds (λ_{ex} = 365 nm) in their solid-state dual emissions were observed in thin film (Fig. S21 and S22). In solid-state, strong intermolecular interactions facilitate rapid internal conversion from higher excited state, resulting emission from S_1 state following Kasha's rule. In thin films, fluorophores are away from one another resulting in weak/no intermolecular interaction and thus, emission from higher excited state is feasible.

19 The ground and first excited states of all the compounds were also optimised using cam-b3lyp functional and 6-311g(d,p) basis set. The molecular orbitals involved in electronic transitions (absorption or emission) are same. However, they largely differ in their energy.

20 (*a*) Y. Zhao, R. Chen, Y. Gao, K. S. Leck, X. Yang, S. Liu, A. P. Abiyasa, Y. Divayana, E. Mutlugun, S. T. Tan, H. Sun, H. V. Demir and X. W. Sun, *Org. Electron.*, 2013, **14**, 3195–3200; (*b*) S. H. Cho, E. H. Kim, B. Jeong, J. H. Lee, G. Song, I. Hwang, H. Cho, K. L. Kim, S. Yu, R. H. Kim, S. W. Lee, T.-W. Leeb and C. Park, *J. Mater. Chem. C*, 2017, **5**, 110–117.

21 (*a*) CCDC 2528322: Experimental Crystal Structure Determination, 2026, DOI: 10.5517/ccdc.csd.cc2qvxs9; (*b*) CCDC 2528323: Experimental Crystal Structure Determination, 2026, DOI: 10.5517/ccdc.csd.cc2qvxtb.